AD-A156 620 ON THE APPLICATION OF COMPATIBILITY CHECKING TECHNIQUES 1/1
TO DYNAMIC FLIGHT TEST DATA(U) AERONAUTICAL RESEARCH
LABS MELBOURNE (AUSTRALIA) R FEIK JUN 84
UNCLASSIFIED ARL-AERO-R-161 F/G 12/1 NL

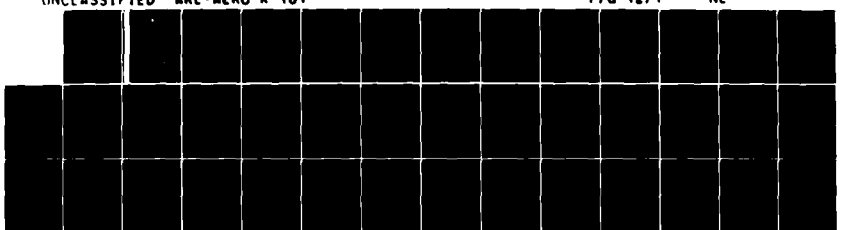

END
DATE FILMED
8-85
DTIC

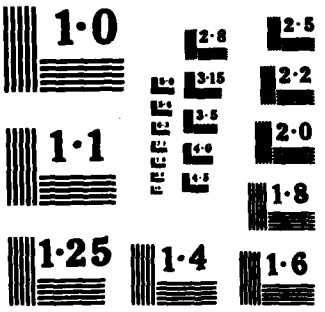
1·0
1·1
1·25
1·4
1·6
1·8
2·0
2·2
2·5
2·8
3·15
3·5

ARL-AERO-R-161

AR-003-931

DEPARTMENT OF DEFENCE

DEFENCE SCIENCE AND TECHNOLOGY ORGANISATION

AERONAUTICAL RESEARCH LABORATORIES

MELBOURNE, VICTORIA

AERODYNAMICS REPORT 161

ON THE APPLICATION OF COMPATIBILITY CHECKING TECHNIQUES TO DYNAMIC FLIGHT TEST DATA

by

R. A. FEIK

Approved for Public Release.

COPY No

JUNE 1984

CONDITIONS OF RELEASE AND DISPOSAL

1. This document is the property of the Australian Government; the information it contains is released for defence purposes only and must not be disseminated beyond the stated distribution without prior approval.
2. The document and the information it contains must be handled in accordance with security regulations applying in the country of lodgement, downgrading instructions must be observed and delimitation is only with the specific approval of the Releasing Authority as given in the Secondary Distribution statement.
3. This information may be subject to privately owned rights.
4. The officer in possession of this document is responsible for its safe custody. When no longer required this document should NOT BE DESTROYED but returned to

   Defence Information Services Branch, Campbell Park, Canberra, ACT 2600 Australia.

AR-003-931

DEPARTMENT OF DEFENCE
DEFENCE SCIENCE AND TECHNOLOGY ORGANISATION
AERONAUTICAL RESEARCH LABORATORIES

AERODYNAMICS REPORT 161

ON THE APPLICATION OF COMPATIBILITY CHECKING TECHNIQUES TO DYNAMIC FLIGHT TEST DATA

by

R. A. FEIK

SUMMARY

This report considers matters related to the application of instrument compatibility checking techniques to flight test data. A previously developed Maximum Likelihood program has been used to study the effects of the presence of scale errors, accelerometer offsets and measurement time lags using simulated data. Some additional information on the effects of noise levels has also been obtained. The results have led to a suggested method for determination of centre of gravity location from flight data. The effects of measurement lags have been shown to have a major influence on extracted instrument parameters and a systematic procedure for the determination of relative phases has been devised and applied successfully to simulated data. These techniques have also been applied to flight data from a roller-coaster manoeuvre and a set of relative lag values clearly identified. The question of the accuracies of extracted instrument parameters and their dependence on the relative lags will be treated more fully in a subsequent publication.

POSTAL ADDRESS: Director, Aeronautical Research Laboratories,
Box 4331, P.O., Melbourne, Victoria, 3001, Australia

CONTENTS

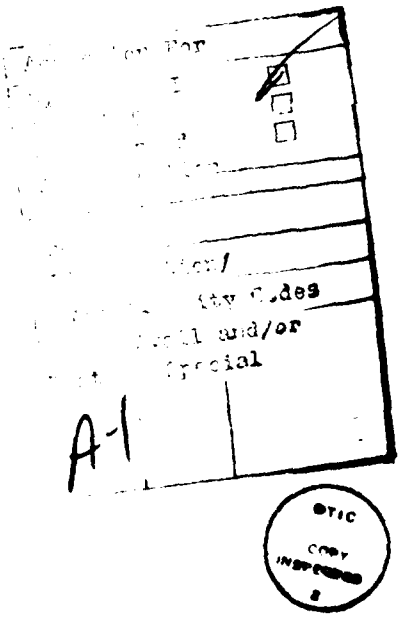

NOTATION

A	Sensitivity matrix, equation (11).
ax, az	Linear accelerations in x, z directions, m/s^2.
b_{ax}, b_{az}, b_q etc.	Offset biases in ax, az, q etc. measurements.
g	Gravitational acceleration, m/s^2.
h	Altitude, m.
i	Time index.
J	Cost functional to be minimized, equation (8).
$\mathbf{n}$	Measurement noise vector, equation (7).
n_{ax}, n_{az}, n_q	Random noise in ax, az, q measurements.
N	Number of time points.
q	Pitch rate, rad/s.
$\mathbf{R}$	Measurement noise matrix.
t	time, sec.
$\mathbf{u}$	Input vector.
u, w	Velocities in x, z directions.
V	Airspeed, m/s.
$\mathbf{x}$	State vector.
$\hat{\mathbf{x}}$	Estimated state vector.
x, z	Reference body axes.
x_α, z_α	Body axis coordinates of angle of attack probe, m.
x_a, z_a	Accelerometer positions relative to centre of gravity, m.
$\mathbf{z}$	Observation vector.
$\hat{\mathbf{z}}$	Calculated observation vector.
α	Angle of attack, radians.
Δ	Increment.
λ_{ax}, λ_{az}, λ_q etc.	Scale factor error in ax, az, q etc. measurements.
θ	Pitch attitude, radians.
ξ	Parameter vector.
σ	Standard deviation.
∇_ξ	Gradient with respect to parameter vector, ξ.

Subscripts

a	Refers to accelerometer location.
cg	Refers to centre of gravity location.
m	Measured values.
out	Output quantities.

1. INTRODUCTION

At ARL, The Aircraft Behaviour Studies–Fixed Wing Group has for some years been active in the application of system identification methodology to the extraction of aerodynamic information from flight test data. The group has acquired or developed a number of parameter and state estimation programs (Ref. 1) and acquired experience in their use and application to flight test data analysis.

The problem of extracting aerodynamic information from dynamic flight test data, especially when the form of the aerodynamic model is uncertain, is compounded by errors in the measurements, particularly systematic bias and scale factor errors. One approach taken seeks to remove instrumentation errors and inconsistencies prior to further analysis, by making use of redundant information available in the quantities measured. This is done by suitably formulating the exact aircraft kinematic equations, relating accelerations, velocities and displacements and including instrument biases and scale factors as unknown parameters. Solutions to the resulting non-linear state and parameter estimation problem have been obtained with simulated data using both Extended Kalman Filter (Ref. 2) and Maximum Likelihood (Ref. 3) methods and a comparison of the two approaches is documented in Reference 4. Both techniques were shown to give acceptable results with simulated data provided certain requirements on manoeuvre shape, noise levels, data length and sampling rate are met. Further development of the Extended Kalman Filter Approach and related techniques has been pursued under a Research Agreement with the University of Newcastle and reported in References 5 and 6. The present report concerns some further results obtained using the Maximum Likelihood technique.

The application of these methods to real as opposed to simulated data introduced elements not considered in References 2 to 4. One of these elements is the location of the accelerometers relative to the aircraft centre of gravity. The location is rarely coincident with the centre of gravity and this introduces certain contributions to the accelerometer readings due to aircraft rotational rates and accelerations. These can be allowed for provided the position of the accelerometer relative to the centre of gravity is known. Alternatively, the kinematic equations can be extended to include these offsets as unknowns to be estimated. The latter approach is developed further in this note. The present study also extends the earlier results by inclusion of calibration slope errors in addition to the bias errors treated in References 2 to 4. This extension as well as the effects of centre of gravity offset errors are initially studied using simulated data.

Another element to be considered with real data is the presence of dynamic lags in the measurement channels. Lags may, for example, be introduced by the signal conditioning electronics. Unless this is identical for each channel it cannot be assumed that the measurements will be precisely in phase. Phase lags of up to around 0·1 second may need to be accounted for. Another source of lag is frequency response limitations in the transducer itself or in the measurement system. This is particularly so with the air data system (e.g. airspeed, altitude) which requires movement of air in and out of reservoirs through tubes of different lengths. Lags introduced in this way may amount to several tenths of a second or more and their influence on the match between calculated and measured time histories and, consequently, on estimated bias and scale factors may be considerable. Provided measurement system frequency response bandwidth is sufficiently wide (typically natural frequency 5 to 10 times the frequency being measured), lags can be approximated by simple time shifts. Lag (or time shift) effects are studied and quantified in this note and a strategy developed, using simulated data, to determine lag values. Some discussion of the effects of lags in airspeed measurement, and also of accelerometer offsets, on estimated parameters can also be found in Reference 6.

In Section 2 of this report the compatibility checking method is reviewed briefly and extensions and modifications relevant to the current investigation are described. Results with these modifications, including centre of gravity location and measurement lag determination using

simulated data, are presented in the next Section. Finally, the techniques developed are applied to flight data.

2. THEORETICAL BACKGROUND

The aircraft kinematic equations of motion, modified to account for centre of gravity offsets, are summarized in this Section. This is followed by a brief theoretical discussion of the Maximum Likelihood (ML) method for solution of the compatibility checking problem and a more detailed treatment of the sensitivity matrix.

2.1 Aircraft Kinematic Equations

The full set of non-linear equations relating the position, velocity and acceleration of an aircraft with reference to a set of flat earth axes is summarized in Reference 3. In the present study only the three degrees of freedom set, representing longitudinal motions, is of interest. The system under consideration may be summarized as follows:

(*i*) State vector, $\mathbf{x} = [u, w, \theta, h]^T$

The state equations written in body axes (x, z) fixed in the aircraft, with origin at the centre of gravity can be considered to be exact (Ref. 7).

$$\left.\begin{aligned} \dot{u} &= -qw + ax_{cg} - g \sin\theta \\ \dot{w} &= qu + az_{cg} + g \cos\theta \\ \dot{\theta} &= q \\ \dot{h} &= u \sin\theta - w \cos\theta \end{aligned}\right\} \tag{1}$$

where

u, w are linear velocities in the x, z directions,

θ, q are pitch attitude and angular rate,

ax_{cg}, az_{cg} are accelerations at the centre of gravity in the x, z directions, and

g is the gravitational constant.

Accelerometers are seldom located exactly at the aircraft centre of gravity. If the accelerometer pack is assumed to be positioned in the plane of symmetry but offset a distance x_a in the x-direction and z_a in the z-direction, then the relationship between the accelerations at the $c.g.$ and those indicated at the accelerometer location, ax_a and az_a, can be written as follows:

$$\left.\begin{aligned} ax_{cg} &= ax_a + q^2 x_a \quad \dot{q} z_a \\ az_{cg} &= az_a + \dot{q} x_a + q^2 z_a \end{aligned}\right\} \tag{2}$$

These non-linear relations require a knowledge of x_a and z_a for evaluation. Alternatively, x_a and z_a may be treated as unknowns and added to the list of parameters to be identified. The latter approach is developed further in this report. In addition, evaluation of Equation (2) requires knowledge of the pitch angular acceleration, $\dot{q}$. This is not normally one of the quantities measured and the present approach is to differentiate records of pitch rate, q, using moving least squares smoothing (Ref. 8) in order to avoid the introduction of phase shifts. This approach gives good

results provided care is taken to optimize the order of fit and the number of points used in the fit, and provided also that noise levels on q are not too high, a condition which is fortunately satisfied due to the quality of pitch rate gyro instrumentation used.

(*ii*) Input vector, $\mathbf{u} = [ax_{CG}, az_{CG}, q]^T$

In the compatibility checking approach, values of ax_{CG}, az_{CG} and q in Equation (1) are treated as inputs. While Equation (2) enables corrections to be made for accelerometer offset relative to the centre of gravity, measured quantities are also subject to errors due to calibration errors, instrument bias errors and random noise. These are modelled as follows:

$$\left.\begin{aligned} ax_a &= (1+\lambda_{ax})ax_m + b_{ax} + n_{ax} \\ az_a &= (1+\lambda_{az})az_m + b_{az} + n_{az} \\ q &= (1+\lambda_q)q_m + b_q + n_q \end{aligned}\right\} \tag{3}$$

where

λ_{ax}, λ_{az} and λ_q represent scale factor errors,

b_{ax}, b_{az} and b_q represent instrument bias errors,

n_{ax}, n_{az} and n_q represent random noise and

subscript m refers to measured values.

When Equations (2) and (3) are substituted into Equation (1) the scale factor and bias errors as well as the accelerometer positions appear explicitly as unknown parameters while the random noise components give rise to process noise. Since accelerometers and gyros are usually the most accurate instruments used in flight testing, the noise levels are in general relatively small and consequently are neglected in the present treatment. This, together with the fact that the state equations can be considered to be exact, ensures that the state equations are free of process noise.

(*iii*) Output vector, $\mathbf{z} = [V, \alpha, \theta, h]^T$

Measurements of the output quantities, viz. airspeed, V, angle of attack, α, pitch attitude, θ and altitude, h, are corrupted by scale factor errors, biases and random noise. The equations used for calculating the outputs are as follows:

$$\left.\begin{aligned} V_{out} &= (1+\lambda_v)(u^2+w^2)^{1/2} + b_v \\ \alpha_{out} &= (1+\lambda_\alpha)\tan^{-1}[(w-qx_\alpha)/u] + b_\alpha \\ \theta_{out} &= (1+\lambda_\theta)\theta + b_\theta \\ h_{out} &= (1+\lambda_h)h + b_h \end{aligned}\right\} \tag{4}$$

The term qx_α/u in the α equation is a correction due to known sensor position, x_α, ahead of the centre of gravity.

The biases, b, and scale factors, λ, in equation (4) are added to the list of unknown parameters introduced previously. Further, the initial conditions of the state equations (1) are also unknown and complete the list of parameters to be determined. The list can be reduced slightly by noting that, since no absolute reference for height, h, is implied in equation (1), the initial height $h(o)$, and bias b_h can be assumed to be zero. The final unknown parameter vector is:

$$\xi = [\lambda_{ax}, b_{ax}, \lambda_{az}, b_{az}, \lambda_q, b_q, \lambda_v, b_v, \lambda_\alpha, b_\alpha, \lambda_\theta, b_\theta, \lambda_h, u(o), w(o), \theta(o), x_a, z_a]^T \tag{5}$$

2.2 Theory

The system described in the previous section form a set of non-linear dynamic equations of the form:

$$\dot{\mathbf{x}}(t) = \mathbf{f}(\mathbf{x}(t), \mathbf{u}(t), \xi) \tag{6}$$

$$\mathbf{z}(i) = \mathbf{g}(\mathbf{x}(i), \mathbf{u}(i), \xi) + \mathbf{n}(i) \tag{7}$$

The measurements, $\mathbf{z}(i)$, are made of a finite number of time points, t_i, and are subject to random measurement noise, $\mathbf{n}$, in addition to the systematic errors represented through the parameter vector, ξ.

Since there is no process noise, an estimate of the state, $\hat{\mathbf{x}}$, is obtained by integration of equation (6) given the estimated value of the parameter vector. Parameter estimation is accomplished using a Maximum Likelihood (ML) method. Assuming that the measurement noise is zero mean uncorrelated and Gaussian, this is equivalent to the minimization of the cost functional (Ref. 9).

$$J(\xi, \mathbf{R}) = \tfrac{1}{2} N \log |\mathbf{R}| + \tfrac{1}{2} \sum_{i=1}^{N} \nu^{\mathrm{T}}(i)\, \mathbf{R}^{-1}\, \nu(i) \tag{8}$$

where $\nu(i) = \mathbf{z}(i) - \mathbf{g}(\hat{\mathbf{x}}(i), \mathbf{u}(i), \xi) = \mathbf{z}(i) - \hat{\mathbf{z}}(\xi, i)$ is the vector of residuals, and $\mathbf{R}$ is a weighting covariance matrix.

An estimate for $\mathbf{R}$ is first obtained by minimizing J (equation(8)) with respect to $\mathbf{R}$, giving

$$\hat{\mathbf{R}} = \frac{1}{N} \sum_{i=1}^{N} \nu(i)\, \nu^{\mathrm{T}}(i) \tag{9}$$

An updated estimate for ξ then follows by minimizing J with respect to ξ. This revised estimate is used for a new estimate of $\mathbf{R}$ and the iteration procedure continued until convergence. The final estimates are asymptotically consistent and efficient with covariance of the estimates approaching the Cramer–Rao bound given by:

$$\text{covariance } (\xi) = \left\{ \sum_{i=1}^{N} \mathbf{A}^{\mathrm{T}}(i)\, \hat{\mathbf{R}}^{-1}\, \mathbf{A}(i) \right\}^{-1} \tag{10}$$

where $\mathbf{A}$ is the sensitivity matrix whose elements are the partial derivatives of the elements of the estimated output vector, $\hat{\mathbf{z}}(\xi, i)$ with respect to elements of the parameter vector, ξ.

$$\mathbf{A}(i) = \nabla_{\xi}(\hat{\mathbf{z}}(\xi, i)) \tag{11}$$

Further details are provided in Reference 3.

2.3 Sensitivity Matrix

A critical part of the ML procedure, both for the parameter estimation and for the calculation of the covariance of the estimates, is the evaluation of the sensitivity matrix. For the current problem the output vector (equation (4)) is of dimension 4 and the parameter vector

(equation (5)) is of dimension 18 resulting in a sensitivity matrix of dimension 4 by 18. The (i, j) element is the partial derivative of the ith component of the output vector with respect to the jth component of the parameter vector. The complete sensitivity matrix, **A**, for the present system is summarized in Appendix 1 and formulae for the evaluation of the various elements given.

In order to evaluate the elements of **A** as functions of time, it can be seen that not only the state u, w, θ, h but also partial derivatives of the state $u_{\xi j}$, $w_{\xi j}$, $\theta_{\xi j}$, $h_{\xi j}$ are required as functions of time, where ξj represents a particular element of the parameter vector. Equations for the required partial derivatives follow from the state equations by first differentiating with respect to ξj and then reversing the order of the partial derivative and the time derivative. The total number of equations, including the state equations, which need to be integrated simultaneously amounts to 39 and these are listed in Appendix 2 together with the relevant initial conditions.

For computing purposes derivative values for all variables to be integrated are evaluated in subroutine DERIVS while manipulations required for calculation of **A** are performed in subroutine SENS. Further details are given in Reference 3. The main program COMPAT is written so that the user may choose any desired subset of the unknown parameters for extraction. The program recognizes the required subset from the input file and makes the necessary adjustments automatically.

3. RESULTS WITH SIMULATED DATA

In this Section the method of the previous Section is used to study those practical aspects described in the introduction. These include in turn, the addition of scale factor errors, accelerometer offset relative to the centre of gravity and the effects of lags in the measurements. Finally, a strategy is developed for the determination of lags and tested using simulated time histories.

3.1 Manoeuvre Description

Two manoeuvre shapes were used in the course of this study, both being representative of roller coaster type of motion in the longitudinal plane, i.e. sequences of pull-ups and push-overs:

Manoeuvre 1 (Fig. 1).—This is similar to the manoeuvre used in Reference 4. Analytical expressions for the inputs ax, az and q are chosen to simulate a real manoeuvre. The higher frequency oscillations, particularly in the pitch rate, q, time history, represents the short period oscillation. Maximum deviations are seen to be about $\pm 0{\cdot}5$ m/s ($0{\cdot}05$ g) for ax, ± 10 m/s (1 g) for az and $\pm 0{\cdot}2$ rad/s (11 deg/s) for q. The corresponding outputs (noise free) used in the current study, namely V, α and θ are also shown in Figure 1.

Manoeuvre 2 (Fig. 2).—The second manoeuvre used is a close representation of a real manoeuvre. Actual measured elevator time histories were used as input to a mathematical model of the aircraft in question and the dynamic response calculations of ax, az and q produced by the model then used as inputs for the current exercise. This manoeuvre, although more realistic than manoeuvre 1, produces somewhat smaller deviations in accelerations and pitch rate.

An auxiliary program was used to add the effects of bias and scale factor errors on measurements of inputs and outputs and of random noise on output measurements. Three different levels of noise have been used at one time or another and these are presented in Table 1 below.

TABLE 1

Noise Standard Errors for Simulated Data

Standard Error	Level 1	Level 2	Level 3
$\sigma(V)$, m/s	1·0	0·1	0·5
$\sigma(\alpha)$, rad	0·002	0·001	0·002
$\sigma(\theta)$, rad	0·01	0·001	0·002

Level 1 represents a high noise case, level 2 low noise and level 3 an intermediate case. Measured outputs shown in Figure 2 represent the level 1 noise case. Also shown in the figure is a time history of pitch acceleration, $\dot{q}$, This has been derived from the pitch rate, q, history by numerical differentiation as explained in Section 2.1. The maximum pitch rate apparent in Figure 2 is approximately 0·08 rad/s while maximum pitch acceleration is about 0·15 rad/s^2. For centre of gravity offsets, x_a and z_a, of say 1 metre these correspond to corrections to accelerometer readings (equation (2)) of 0·006 m/s^2 and 0·15 m/s^2 respectively. Clearly the $\dot{q}$ contributions are dominant and can make significant contributions to the u and w state equations, comparable at times to the contributions of the bias terms, b_{ax} and b_{az}, which are set at 0·1 m/s^2 in the simulated runs of the following Section.

3.2 Results with Scale Factor Errors and Accelerometer Offsets

All simulation results reported in this and the next Section were obtained using 40 seconds of record at 40 samples per second, shown to give satisfactory results in References 3 and 4. CPU time on the DEC-System 10 computer for 10 iterations of the minimizing procedure was typically 20 minutes, varying only slightly with the number of parameters extracted. Only the three outputs V, α and θ were matched since Reference 3 suggests that relatively minor improvements are obtained by the addition of height h, as an output.

The results including scale factor and accelerometer offset extraction are summarized in Tables 2 and 3 . The full parameter vector considered here is:

$$\xi = [b_{ax}, b_{az}, \lambda_q, b_q, \lambda_v, b_v, \lambda_z, b_z, b_\theta, u(o), w(o), \theta(o), x_a, z_a]$$

and includes the scale factors λ_q, λ_v, λ_z and accelerometer offsets x_a, z_a. Normally scale factor errors for gyros and accelerometers can be expected to be small, although in the current exercise λ_q has been retained due to inconsistencies noted in the pitch rate gyro calibrations for the flight-data to be considered in Section 4. A priori estimates for all parameters except the initial conditions were set to zero. Initial condition estimates were derived from the simulated outputs.

The results in Table 2 were extracted using manoeuvre 2 and low noise levels. In the first column no accelerometer offsets are present but all other parameters are included. Most parameters are well identified and the Cramer–Rao bounds (in brackets) are good indicators of their accuracy as noted in References 3 and 4. It is particularly pleasing that the scale factors λ_q, λ_v and λ_z are very precisely identified and present no special problems. The second column includes accelerometer offsets of $\pm$ 1 m in both the x and z directions. Their inclusion leads to no noticeable deterioration in the accuracy of the other parameters. However, while x_a and z_a are

reasonably well identified the accuracy, particularly of x_a, as indicated by the Cramer–Rao bound, is relatively poor. This is most probably associated with the small overall contributions the $\dot{q}$ terms make in the equations of motion for this manoeuvre, compared to the other bias and scale factor errors. The absence of other errors can lead to an improvement in accuracy for x_a and z_a as shown in column 3 of Table 2.

TABLE 2

Results with Scale Errors and C.G. Offsets

Parameter	True value	1	2	3
b_{ax}, m/s^2	0·1	0·114 (0·003)	0·095 (0·003)	0·098 (0·003)
b_{az}, m/s^2	0·1	0·102 (0·0007)	0·100 (0·0007)	—
λ_q	0·01	0·0098 (0·0002)	0·0101 (0·0002)	—
b_q, rad/s	0·002	0·0020 (0·000002)	0·0020 (0·000002)	—
λ_v	0·1	0·100 (0·0003)	0·099 (0·0004)	—
b_v, m/s	1·0	0·82 (0·07)	1·16 (0·08)	1·02 (0·03)
λ_α	0·1	0·099 (0·0005)	0·100 (0·0007)	—
b_α, rad	0·002	0·0022 (0·0002)	0·0020 (0·0002)	—
b_θ, rad	0·01	0·0086 (0·0003)	0·0105 (0·0003)	0·0102 (0·0003)
$u(o)$, m/s	193·76	193·89 (0·04)	193·74 (0·05)	193·74 (0·03)
$w(o)$, m/s	28·85	28·88 (0·02)	28·85 (0·02)	28·85 (0·01)
$\theta(o)$, rad	0·148	0·148 (0·003)	0·147 (0·0003)	0·148 (0·0003)
x_a, m	−1·0	—	−0·90 (0·20)	−1·04 (0·13)
z_a, m	1·0	—	0·97 (0·09)	1·05 (0·07)

Manoeuvre 2; Noise Level 2.

Alternatively, the accuracy of extraction of x_a and z_a can be improved by increasing the contributions of the $\dot{q}$ terms. There is considerable scope for [illegible]g this since the manoeuvres studied here are relatively mild. Thus a manoeuvre with large rate accelerations could provide a method for obtaining aircraft centre of gravity position directly from flight tests. This requires further investigation but is not pursued here.

Table 3 presents some results showing the effects of bias and scale factor magnitudes and random noise levels on the accuracy of extraction of the various parameters. The first two columns both have level 2 (low) noise but bias and scale factor errors are twice as large in the first column as in the second. The Cramer–Rao bounds, determined principally by the noise level, are identical in both cases and most parameters are identified equally well. A possible exception is b_v and more particularly x_a, accelerometer offset in the x-direction. Both of these appear to be biased in the first column in the sense that their deviations from the true values are well outside the predicted Cramer–Rao error bounds.

Columns 2, 3 and 4 of Table 3 compare results with low, high and intermediate noise levels respectively, but with the lower bias and scale factor errors. The deterioration in accuracy, in particular the Cramer–Rao bound, as noise levels increase is obvious. In column 4 the results are the mean of eight separate runs and the standard deviations are closely approximated by the Cramer–Rao bounds.

In summary, this Section has shown that the presence of scale factors does not present any difficulties to the compatibility checking algorithm, which is capable of calculating their values with very good accuracy. For the relatively mild manoeuvre considered, the accelerometer offsets were only identified with moderate accuracy, however the presence of offsets did not

TABLE 3

Influence of Error Magnitude and Noise Level

Parameter	True Value	1	2	3	4
b_{ax},m/s^2	0·2/0·1	0·190 (0·003)	0·095 (0·003)	0·092 (0·018)	0·112 (0·010)
b_{az},m/s^2	0·2/0·1	0·200 (0·0007)	0·100 (0·0007)	0·091 (0·0044)	0·101 (0·0015)
λ_q	0·1/0·05	0·100 (0·0002)	0·050 (0·0002)	0·052 (0·0015)	0·050 (0·0003)
b_q,rad/s	0·004/0·002	0·0040 (0·000002)	0·0020 (0·000002)	0·0020 (0·00002)	0·0020 (0·000005)
λ_v	0·1/0·05	0·100 (0·0004)	0·050 (0·0004)	0·055 (0·0033)	0·050 (0·002)
b_v,m/s	1·0/0·5	0·75 (0·08)	0·48 (0·08)	−0·09 (0·7)	0·40 (0·3)
λ_α	0·1/0·05	0·099 (0·0007)	0·049 (0·0007)	0·051 (0·0021)	0·050 (0·002)
b_α,rad	0·004/0·002	0·0042 (0·0002)	0·0021 (0·0002)	0·0024 (0·0010)	0·0019 (0·0006)
b_θ,rad	0·004/0·002	0·0050 (0·0003)	0·0025 (0·0003)	0·0024 (0·0018)	0·0012 (0·0010)
$u(o)$,m/s	193·76	193·91 (0·05)	193·81 (0·05)	193·32 (0·29)	193·78 (0·12)
$w(o)$,m/s	28·85	28·85 (0·02)	28·84 (0·02)	28·70 (0·17)	28·89 (0·10)
$\theta(o)$,rad	0·148	0·147 (0·0003)	0·147 (0·0003)	0·146 (0·002)	0·149 (0·001)
x_a,m	−1·0	−0·51 (0·2)	−0·90 (0·2)	−1·56 (0·5)	−1·12 (0·5)
z_a,m	1·0	1·08 (0·09)	1·05 (0·09)	1·88 (0·9)	1·01 (0·4)
Noise Level		2	2	1	3

Manoeuvre 2.

have any adverse effects on the other parameters. Finally, increases in noise levels lead to significant degradation in accuracy but increased bias and scale factor magnitudes do not in general affect the relative accuracy of the identified values.

3.3 Results with Lags

The questions addressed in this Section include what the effects of lags are on the identified parameter values and how measurement lags affect the fit errors between calculated and measured time histories. In order to answer these questions a systematic study was carried out whereby a lag of $\pm$ 0·05 s was imposed on each of the inputs (ax, az, q) and outputs (V, α, θ) in turn. For this study level 2 (low) noise level was used and the parameter vector was:

$$\xi = [b_{ax}, b_{az}, \lambda_q, b_q, b_V, b_\alpha, b_\theta, u(o), w(o), \theta(o)]$$

Both manoeuvres 1 and 2 were used and, as may be expected, the main parameters to be affected were those that were found to be least accurately determined in the previous Section (also see Ref. 3), viz. b_{ax}, b_V, b_α and b_θ. The results are presented qualitatively in Table 4 below, where a major change (100% or more) in a parameter is denoted by a large × while a relatively

TABLE 4

Effects of Lags on Identified Parameters

Lag in \ Parameter	b_{ax}	b_V	b_α	b_θ
ax				
az	×	+		×
q	×	×	×	×
V	+		×	+
α	+	×		+
θ	+	+	+	

Manoeuvre 1, 2; Noise Level 2.

minor change is indicated by a small +. Thus a lag of 0·05 second in az leads to major changes in b_{ax} and b_θ and a small but significant change in b_V. Note that there are only two major changes in each column and they are in general of opposite sign. For example b_{ax} is strongly affected by a lag in az and similarly affected, in the opposite direction, by a lag in q. This suggests that the main influence of b_{ax} is the relative phase between az and q. Similarly for b_θ while for b_V the phase between q and α is important and for b_α, that between q and V. Thus a lag in q affects all four parameters in a major way, a lag in az affects b_{ax} and b_θ, while lags in V and α influence only b_α and b_V respectively. A lag in ax has no noticeable effect on any parameter and a lag in θ affects b_{ax}, b_V and b_α in a minor way.

Results showing the influence of lags on the V, α and θ fit errors are summarized in Table 5. The numbers relate to manoeuvre 2 and are weighted RMS fit errors obtained after 5 iterations of the minimization algorithm. For no lags, values close to 1 would be obtained in all cases. Small variations may be expected due to differences in the random noise sequences used in each case. The results show clearly that the fit error for V is affected only by the relative phase of q and V while the θ-fit depends on the relative phase of q and θ. The α-fit on the other hand is influenced by the relative phases of q, az and α. Once again the q lag appears to be dominant while ax lag has no discernible effect on the fit errors. On the other hand θ lag with respect to q,

TABLE 5

Fit Errors Obtained After 5 Iterations

0·05 s Lag in	V-fit	α-fit	θ-fit
ax	1·03	1·01	1·01
az	1·04	1·47	1·04
q	1·33	2·41	4·30
V	1·25	0·98	1·01
α	0·96	1·94	1·03
θ	1·01	0·93	4·48

Manoeuvre 2; Noise Level 2.

while influencing some parameters in a minor way (Table 4), has a large effect on the θ-fit. At the same time V lag w.r.t. q has a significant influence on the V-fit corresponding with its effect on b_α in Table 4. Finally, Table 4 suggests that the relative phase of az and α is relatively unimportant so that the α-fit results in Table 5 can be assumed to reflect $q-az$ and $q-\alpha$ phase differences independently, the $\alpha-az$ phase relationship being of secondary importance. These observations lead to the following strategy for determining relative phases:

1. Take q as reference signal.
2. Align θ with q by minimizing θ-fit w.r.t. θ lag.
3. Align α with q by minimizing α-fit w.r.t. α lag.
4. Align az with q by minimizing α-fit w.r.t. az lag.
5. Align V with q by minimizing V-fit w.r.t. V lag.

The above steps 2 to 5 can be iterated to check possible coupling effects. In particular repetition of steps 3 and 4 can be repeated to confirm that az and α can be independently aligned with q and that the relative alignment of $az-\alpha$ is unimportant.

In order to check the above strategy a set of manoeuvre 1 time histories with level 1 (high) noise was generated and then shifted relative to one another to produce the relative lags shown in Table 6. The parameter vector used in this simulation included the scale factors λ_v and λ_a.

TABLE 6

Relative Lags

Lag in	Seconds	Sample intervals
ax	0·05	2
az	0·05	2
q	0	0
V	0·275	11
α	−0·1	−4
θ	−0·05	−2

but not λ_q, together with biases and initial conditions as before. Starting with step 2 of the strategy, the θ record was systematically shifted and each time the compatibility checking program used to match records. The shift which produced the least θ-fit error after five iterations of the algorithm established the relative lag of the θ record with respect to the q reference. This same general procedure was repeated for the α-record (step 3) and so on. At each stage the appropriate time history was shifted by the identified number of lag time intervals before proceeding to the next step.

The results of the above procedure are summarized in Figures 3 and 4. In Figure 3 the minimum point of the θ-fit error identifies the correct θ lag value (−2) and similarly the α-fit error identifies the α lag value (−4). Also shown are the variations in the other fit errors as θ lag or α lag are varied. As expected, these variations are small by comparison. In Figure 4 (upper) the correct az lag value (2) is obtained by minimizing the α-fit error with respect to az lag. It can be assumed that ax lag is the same as az lag although, as noted earlier, the value of ax lag does not significantly affect the results. Finally, Figure 4 (lower) determines V lag (11) by minimizing the V-fit error with respect to V lag. Both minima in Figure 4 are weaker than those shown in Figure 3, but the lag values are, nevertheless, unambiguously identified. With the determination of V lag the process is complete and examination of Figures 3 and 4 shows that the final correct set of lags corresponds to the absolute minimum fit errors for each of the θ, α and V fits. Further, it has not been found necessary to iterate the procedure.

These results with simulated data show that it is possible to determine lag values accurately by systematic shifting of input and output time histories using the q history as reference. Quantitative differences may occur with different manoeuvre shapes but the present results show good qualitative agreement in results from manoeuvre 1 (Figures 3 and 4) and manoeuvre 2 (Table 5).

4. LAG RESULTS WITH FLIGHT DATA

The practical considerations studied in the previous Section are applied here to data obtained, on an opportunity basis, during performance flight trials of a delta wing fighter aircraft by the RAAF Aircraft Research and Development Unit (ARDU). The manoeuvre and data acquired will first be described followed by discussion of some of the steps required in preparation for application of the compatibility checking program. The results for instrumentation lag will then be presented.

4.1 Manoeuvre and Data Acquisition

The manoeuvre under consideration is a roller coaster manoeuvre commencing at an altitude of approximately 33 000 ft and a Mach number of 0·65. Lateral motions were minimal so that the manoeuvre could be considered to be purely longitudinal. Flight test instrumentation included a pitch rate gyro, pitch attitude gyro and accelerometers to measure normal and axial accelerations. A nose-probe fitted with a hemispherical, 5-port flow angle sensor was used for angle of attack measurements. This design placed pressure transducers within the probe and as close to the probe head as possible, thereby reducing time lags due to the tubing to negligible amounts. The probe was calibrated in the ARL transonic wind tunnel. Airspeed measurements were only available through the aircraft air data system and presumably subject to significant time lags. Finally, pressure altitude, although not used in determining lags, was also available.

Data were digitally recorded (12 bit accuracy) on magnetic tape via the Aircraft Flight Test Recording and Analysis System (AFTRAS—Ref. 10) used by ARDU, at a sampling rate of 60 per second. Instrument lags and lags introduced by the data conditioning prior to recording were unknown. Copies, on seven track tape, of the ARDU flight tapes were provided to ARL and processed as described in Reference 11 to obtain the required time histories in Engineering units. Time histories for the manoeuvre under consideration are shown in Figure 5. The roller coaster motion during the 40 seconds of flight shown is apparent, with an initial decrease in airspeed as the aircraft climbs followed by an increase as the aircraft descends and so on. Pitch dampers were not operating during this flight as evidenced by the short period oscillations particularly noticeable in the az, q and α records.

From Figure 5 it can be seen that the range of values of ax is relatively small spanning about $\pm$ 0·3 m/s² (0·03 g). Meanwhile the range of the az measurements is around $\pm$ 10 m/s² (1 g) and q spans approximately $\pm$0·11 rad/s (6 deg/s). These values represent a relatively gentle manoeuvre. Noise of the q and az measurements is not discernible on the traces while that on ax appears to be confined to a range of $\pm$ 0·05 m/s² (0·005 g). Larger scale plots suggest a similar noise level (0·05 m/s²) on az and $\pm$0·002 rad/s (0·1 deg/s) on q. Noise is much more obvious on the V and h outputs being about $\pm$ 1 m/s (2 knots) and $\pm$ 25 ft (8 m) respectively. However, for α and θ, noise is difficult to estimate on the scales given, but from larger scale plots random noise was estimated to be at most $\pm$ 0·002 rad (0·1°) for the α and θ records. Noise bandwidth was unknown in all cases.

4.2 Preliminary Calculations

The pitch rate acceleration, $\dot{q}$, required in order to take into account accelerometer offset from centre of gravity was calculated by numerical differentiation using a moving least squares fit as explained in Section 2.1. Some experimentation was necessary with the number of points smoothed and the order of the polynomial fit required to obtain smoothly varying results. Figure 6 shows the original pitch rate time history, q, and the pitch acceleration record, $\dot{q}$, as derived using a fourth order polynomial smoothing 40 points at a time. The results appear to be quite satisfactory.

A priori estimates of the accelerometer offsets relative to the c.g. were made using the known position of the accelerometers and calculated values of the c.g. location. The latter were obtained using a mathematical model of the aircraft (Ref. 12), given the aircraft configuration, initial weight and fuel gone. This resulted in an estimate for x_a of - 0·11 and for z_a of 0·53 m.

The output vector in the compatibility checking program included V, α and θ but not h. The diagonal weighting matrix, $\mathbf{R}$, in equation (8), was based on noise standard deviations of 1 m/s for V and 0·001 rad for α and θ. These values were not varied during the 5 iterations of the program used at each step of the lag determination process. The results have been found to be relatively insensitive to the value of the $\mathbf{R}$ matrix. The parameter vector used reflects anticipated systematic errors based on calibration information provided by ARDU. In particular

the scale factor error λ_q is included since separate calibrations were found to produce significant differences in pitch rate gyro calibration slope. The complete vector was:

$$\xi = [b_{ax},\ b_{az},\ \lambda_q,\ b_q,\ \lambda_v,\ b_v,\ \lambda_\alpha,\ b_\alpha,\ \lambda_\theta,\ b_\theta,\ u(o),\ w(o),\ \theta(o),\ x_a,\ z_a]^T$$

It was noted also that x_a and z_a were not important in the current manoeuvre since relatively small pitch rates and accelerations were present. Consequently, to avoid x_a and z_a taking up unrealistic values, a priori weightings were specified based on standard deviations of 0·5 and 0·2 m for x_a and z_a respectively. All other parameters were allowed to vary without any a priori weighting. In some cases it was found that the presence of a priori weights on parameters could distort the result.

4.3 Determination of Lags

The results using the procedure outlined in Section 3.3 are shown in Figures 7 and 8 and can be compared with the corresponding results with simulated data in Figures 3 and 4. Note that the lag values identified in Figures 7 and 8 must be compared with the reference q lag value, which, for practical reasons, is 6 rather than zero.

As with the simulated data, the flight data (Fig. 7) shows the θ and α fit errors to be strong functions of θ lag and α lag respectively. The θ lag value is close to 8 and the α lag value is 3. Given that the reference q lag is 6, this means that the α signal leads the q signal by 3 sample intervals or 0·05 seconds. This is not entirely surprising in view of the probe design as discussed in Section 4.1. Differences between q and α lag values can be ascribed to transducer characteristics and signal conditioning. In Figure 8 the variations of α and V fit errors with az lag and V lag respectively are relatively weak but nevertheless, as with the simulated data of Figure 4, clear minima can be discerned. Thus the az lag value is about 12 while the V lag value is about 28. It may be conjectured that a more violent manoeuvre leading to more rapid variations in aircraft state would result in a more pronounced minimum in the V fit curve. This has yet to be tested. The present results show that lags can be identified from flight data in a straight forward, systematic manner. As with the simulated data, iteration of the procedure was not needed.

The length of data required to achieve good results would depend on the information present in the available data, i.e. the manoeuvre shape. In the present instant, increasing the data length to 70 s made little difference to the identified lags. However variations, particularly of α fit error with az lag, were somewhat weaker. This suggests that shorter data lengths would be satisfactory in identifying the lags, although the accuracy of the parameters extracted would deteriorate with reduced record length (Ref. 3). The accuracy of extraction of the unknown instrumentation parameters and their dependence on measurement lags will be addressed in a subsequent note.

Finally, the match achieved after 5 iterations between the calculated and measured histories of V, α and θ, with all lags adjusted in accordance with their values determined as above, is shown in Figure 9. For α and θ the calculated and measured responses are almost indistinguishable with root mean square fit errors of 0·0016 and 0·0022 radians respectively. The error in the V match is more discernible with a root mean square value of 0·61 m/s. The measured V record also shows hints of flatness at its peak and valley, indicating possible friction or deadband effects in the air data computer. Such non-linear effects have not been included in the model and may possibly influence the identified lag values. Ideally, the ability of the suggested procedure to identify lag values correctly should be verified against independent experimentally determined values.

5. CONCLUDING REMARKS

Several matters relating to the application of instrument compatibility checking techniques to real data have been studied in this report. These include the presence of calibration or scale errors in addition to bias errors, accelerometer offsets relative to aircraft centre of gravity, and

relative phase or time shifts between the measurements. Only symmetric motions of the aircraft were considered.

The compatibility checking method reformulates the aircraft kinematic equations so as to make use of the redundant information available in the measurements to extract information about the instrument systematic errors and accelerometer offsets. A Maximum Likelihood program is used to solve the resulting non-linear estimation problem. Neglect of process noise is justified because of the exactness of the kinematic equations and the low noise on the measured inputs.

The results with simulated data demonstrated that the compatibility checking algorithm was capable of calculating scale factor errors to very good accuracy even at high noise levels, although some general degradation of accuracy with increased measurement noise was evident. On the other hand, for the relatively mild manoeuvres considered, accelerometer offsets were only identified to moderate accuracy. However, with manoeuvres designed to produce large rate accelerations the present technique offers the potential of in-flight determination of centre of gravity axial and vertical location and may be worth investigating further.

Simulated manoeuvres also demonstrated that relatively small phase shifts between measured time histories can have major effects on the values of extracted parameters and also on the match achieved between calculated and measured data. The latter effect was used to devise a systematic procedure to identify the unknown relative phases. The procedure was applied successfully to simulated records.

The lag determination procedure was also applied to a 40-second segment of flight data representative of a roller-coaster manoeuvre. The compatibility checking program in this case made allowance for calibration and bias errors and also for accelerometer offset. The instrumentation was of moderately good accuracy and, for the given manoeuvre shape and length, a credible set of lag values was clearly identified. In particular, the airspeed measurement lagged the reference pitch rate measurement by 22 lag intervals or approximately 0·37 seconds. A check against an independent, experimentally determined value would be highly desirable.

It must be emphasized that the instrument error model used assumes linear calibrations with constant bias and scale factor errors and excludes such effects as non-linear or Mach number dependent calibrations, friction or deadband effects and so on. While these assumptions are probably reasonable for the manoeuvre considered, the assumption of invariance with Mach number of airspeed and angle of attack calibrations may be doubtful at transonic speeds, implying that speed ranges should be kept to a minimum, a condition unfavourable to lag determination. Thus regions of non-linear calibrations should be avoided as far as possible to ensure accuracy of the procedure.

The question of the accuracy of the extracted parameters has only been treated briefly and this important question, including the effect of lags on the parameter values, will be addressed more fully in a subsequent report.

REFERENCES

1. Feik, R. A. — Estimation Programs for Dynamic Flight Test Data Analysis. ARL Aero Tech. Memo. 344, January 1983.

2. Martin, C. A. — Estimation of Aircraft Dynamic States and Instrument Systematic Errors from Flight Test Measurements Using the Carlson Square Root Formulation of the Kalman Filter. ARL Aero Note 399, September 1980.

3. Feik, R. A. — A Maximum Likelihood Program for Non-Linear System Identification with Application to Aircraft Flight Data Compatibility Checking. ARL Aero Note 411, July 1982.

4. Martin, C. A., and Feik, R. A. — Estimation of Aircraft Dynamic States and Instrument Systematic Errors from Flight Test Measurements. I.E. Aust., Second Conference on Control Engineering, Newcastle, 25–27 August 1982.

5. De Souza, C. E., Evans, R. J., and Goodwin, G. C. — Non-linear Estimation Algorithms for Flight Path Reconstruction. University of Newcastle, Department of Electrical and Computer Engineering, Technical Report EE8316, March 1983.

6. Norton, J. P., De Souza, C. E., Evans, R. J., and Goodwin, G. C. — Non-linear Estimation Algorithms for Aircraft Flight Path Reconstruction. University of Newcastle, Department of Electrical and Computer Engineering, Technical Report EE8340, October 1983.

7. Etkin, B. — Dynamics of Atmospheric Flight. John Wiley and Sons, 1972.

8. Gilbert, N. E. — The Use of Recursive Expressions in Modifying Least Squares Estimates in Response to the Addition or Removal of an Observation. WRE Tech. Memo. 56 (WR & D), March 1971.

9. Goodwin, G. C., and Payne, R. L. — Dynamic System Identification: Experiment Design and Data Analysis. Academic Press, 1977.

10. ——— — Aircraft Flight Test Recording and Analysis System (AFTRAS). ARDU TN Gen 11, November 1977.

11. Drobik, J. S. — Procedures for Processing AFTRAS Flight Data Tapes from ARDU. ARL Aero Tech. Memo. 348, February 1983.

12. Rein, J. A., Barrett, J. E., and Wilson, R. — Description of Six Degree of Freedom Rigid Aircraft Mathematical Model. WRE-TN-901 (WR & D), March 1973.

APPENDIX 1

Sensitivity Matrix (SENS)

The parameter vector has dimension 18 (equation (5)):

$$\xi = [\lambda_{ax}, b_{ax}, \lambda_{az}, b_{az}, \lambda_q, b_q, \lambda_v, b_v, \lambda_\alpha, b_\alpha, \lambda_\theta, b_\theta, \lambda_h, u(o), w(o), \theta(o), x_a, z_a]^T$$

and the output vector has dimension 4 (equation (4)):

$$\hat{z} = [V_{out}, \alpha_{out}, \theta_{out}, h_{out}]^T$$

It follows that the 4×18 sensitivity matrix **A** is defined by:

$$\mathbf{A}^T = \begin{array}{c|cccc} \hat{z} \rightarrow & V_{out} & \alpha_{out} & \theta_{out} & h_{out} \\ \xi \downarrow & & & & \\ \hline \lambda_{a_x} & V_{out,\lambda ax} & \alpha_{out,\lambda ax} & 0 & h_{out,\lambda ax} \\ b_{a_x} & V_{out,b ax} & \alpha_{out,b ax} & 0 & h_{out,b ax} \\ \lambda_{a_z} & V_{out,\lambda az} & \alpha_{out,\lambda az} & 0 & h_{out,\lambda az} \\ b_{a_z} & V_{out,b az} & \alpha_{out,b az} & 0 & h_{out,b az} \\ \lambda_q & V_{out,\lambda q} & \alpha_{out,\lambda q} & \theta_{out,\lambda q} & h_{out,\lambda q} \\ b_q & V_{out,b q} & \alpha_{out,b q} & \theta_{out,b q} & h_{out,b q} \\ \lambda_v & (u^2+w^2)^{1/2} & 0 & 0 & 0 \\ b_v & 1 & 0 & 0 & 0 \\ \lambda_\alpha & 0 & \tan^{-1} f_1 & 0 & 0 \\ b_\alpha & 0 & 1 & 0 & 0 \\ \lambda_\theta & 0 & 0 & \theta & 0 \\ b_\theta & 0 & 0 & 1 & 0 \\ \lambda_h & 0 & 0 & 0 & h \\ u(o) & V_{out,u(o)} & \alpha_{out,u(o)} & 0 & h_{out,u(o)} \\ w(o) & V_{out,w(o)} & \alpha_{out,w(o)} & 0 & h_{out,w(o)} \\ \theta(o) & V_{out,\theta(o)} & \alpha_{out,\theta(o)} & (1+\lambda_\theta) & h_{out,\theta(o)} \\ x_a & V_{out,x_a} & \alpha_{out,x_a} & 0 & h_{out,x_a} \\ z_a & V_{out,z_a} & \alpha_{out,z_a} & 0 & h_{out,z_a} \end{array}$$

where

$$f_1 = \{w - [(1+\lambda_q)q_m + b_q]x_\alpha\}/u$$

and

$$V_{out,\xi_j} = (1+\lambda_v)(u \cdot u_{\xi_j} + w \cdot w_{\xi_j})/(u^2+w^2)^{1/2}$$

$$\alpha_{out,\xi_j} = (1+\lambda_\alpha)(w_{\xi_j} - f_1 \cdot u_{\xi_j})/u(1+f_1^2)$$

$$\theta_{out,\xi_j} = (1+\lambda_\theta)\theta_{\xi_j}$$

$$h_{out,\xi_j} = (1+\lambda_h)h_{\xi_j}.$$

These relationships hold in general for those elements ξ_j of the parameter vector as listed above in the sensitivity matrix. The only exceptions are:

$$\alpha_{out,\lambda q} = (1+\lambda_\alpha)(w_{\lambda q} - f_1 \cdot u_{\lambda q} - q_m \cdot x_\alpha)/u(1+f_1^2)$$

$$\alpha_{out,b q} = (1+\lambda_\alpha)(w_{b q} - f_1 \cdot u_{b q} - x_\alpha)/u(1+f_1^2).$$

APPENDIX 2

Differential Equations (DERIVS)

In order to calculate the state (equation (1)) and the elements of the sensitivity matrix (Appendix 1) the following system of 39 simultaneous ordinary differential equations needs to be integrated with respect to time:

$$\dot{u} = -f_2 \cdot w + [(1+\lambda_{ax})ax_m + b_{ax}] + f_2^2 \cdot x_a - (1+\lambda_q)\dot{q}_m z_a - g \sin\theta$$

$$\dot{w} = f_2 \cdot u + [(1+\lambda_{az})az_m + b_{az}] + f_2^2 \cdot z_a + (1+\lambda_q)\dot{q}_m x_a + g \cos\theta$$

$$\dot{\theta} = f_2$$

$$\dot{h} = u \sin\theta - w \cos\theta$$

$$\dot{u}_{\lambda_{ax}} = -f_2 \cdot w_{\lambda_{ax}} + ax_m$$

$$\dot{w}_{\lambda_{ax}} = f_2 \cdot u_{\lambda_{ax}}$$

$$\dot{h}_{\lambda_{ax}} = u_{\lambda_{ax}} \cdot \sin\theta - w_{\lambda_{ax}} \cdot \cos\theta$$

$$\dot{u}_{b_{ax}} = f_2 \cdot w_{b_{ax}} + 1$$

$$\dot{w}_{b_{ax}} = f_2 \cdot u_{b_{ax}}$$

$$\dot{h}_{b_{ax}} = u_{b_{ax}} \cdot \sin\theta - w_{b_{ax}} \cdot \cos\theta$$

$$\dot{u}_{\lambda_{az}} = -f_2 \cdot w_{\lambda_{az}}$$

$$\dot{w}_{\lambda_{az}} = f_2 \cdot u_{\lambda_{az}} + az_m$$

$$\dot{h}_{\lambda_{az}} = u_{\lambda_{az}} \cdot \sin\theta - w_{\lambda_{az}} \cdot \cos\theta$$

$$\dot{u}_{b_{az}} = -f_2 \cdot w_{b_{az}}$$

$$\dot{w}_{b_{az}} = f_2 \cdot u_{b_{az}} + 1$$

$$\dot{h}_{b_{az}} = u_{b_{az}} \cdot \sin\theta - w_{b_{az}} \cdot \cos\theta$$

$$\dot{u}_{\lambda_q} = -f_2 \cdot w_{\lambda_q} - w \cdot q_m - g \cos\theta \cdot \theta_{\lambda_q} + 2f_2 \cdot q_m x_a - \dot{q}_m z_a$$

$$\dot{w}_{\lambda_q} = f_2 \cdot u_{\lambda_q} + u \cdot q_m - g \sin\theta \cdot \theta_{\lambda_q} + \dot{q} x_a + 2f_2 \cdot q_m z_a$$

$$\dot{\theta}_{\lambda_q} = q_m$$

$$\dot{h}_{\lambda_q} = u_{\lambda_q} \cdot \sin\theta - w_{\lambda_q} \cdot \cos\theta + (u\cos\theta + w\sin\theta)\theta_{\lambda_q}$$

$$\dot{u}_{b_q} = -f_2 \cdot w_{b_q} - w - g\cos\theta \cdot \theta_{b_q} + 2f_2 \cdot x_a$$

$$\dot{w}_{b_q} = f_2 \cdot u_{b_q} + u - g\sin\theta \cdot \theta_{b_q} + 2f_2 \cdot z_a$$

$$\dot{\theta}_{b_q} = 1$$

$$\dot{h}_{b_q} = u_{b_q} \cdot \sin\theta - w_{b_q} \cdot \cos\theta + (u\cos\theta + w\sin\theta)\theta_{b_q}$$

$$\dot{u}_{u(o)} = -f_2 \cdot w_{u(o)}$$

$$\dot{w}_{u(o)} = f_2 \cdot u_{u(o)}$$

$$\dot{h}_{u(o)} = u_{u(o)} \cdot \sin\theta - w_{u(o)} \cdot \cos\theta$$

$$\dot{u}_{w(o)} = -f_2 \cdot w_{w(o)}$$

$$\dot{w}_{w(0)} = f_2 \,.\, u_{w(0)}$$

$$\dot{h}_{w(0)} = u_{w(0)} \,.\, \sin\theta - w_{w(0)} \,.\, \cos\theta$$

$$\dot{u}_{\theta(0)} = -f_2 \,.\, w_{\theta(0)} - g\cos\theta$$

$$\dot{w}_{\theta(0)} = f_2 \,.\, u_{\theta(0)} - g\sin\theta$$

$$\dot{h}_{\theta(0)} = u_{\theta(0)} \,.\, \sin\theta - w_{\theta(0)} \,.\, \cos\theta + (u\cos\theta + w\sin\theta)$$

$$\dot{u}_{x_a} = -f_2 \,.\, w_{x_a} + f_2^2$$

$$\dot{w}_{x_a} = f_2 \,.\, u_{x_a} + (1+\lambda_q)\dot{q}_m$$

$$\dot{h}_{x_a} = u_{x_a} \,.\, \sin\theta - w_{x_a} \,.\, \cos\theta$$

$$\dot{u}_{z_a} = -f_2 \,.\, w_{z_a} - (1+\lambda_q)\dot{q}_m$$

$$\dot{w}_{z_a} = f_2 \,.\, u_{z_a} + f_2^2$$

$$\dot{h}_{z_a} = u_{z_a} \,.\, \sin\theta - w_{z_a} \,.\, \cos\theta$$

where

$$f_2 = (1+\lambda_q)q_m + b_q.$$

Initial conditions are zero for all variables with the exception of the states $u(o)$, $w(o)$, $\theta(o)$ which are among the parameters to be estimated, and the two variables $u_{u(0)}$ and $w_{w(0)}$ which are initially 1·0.

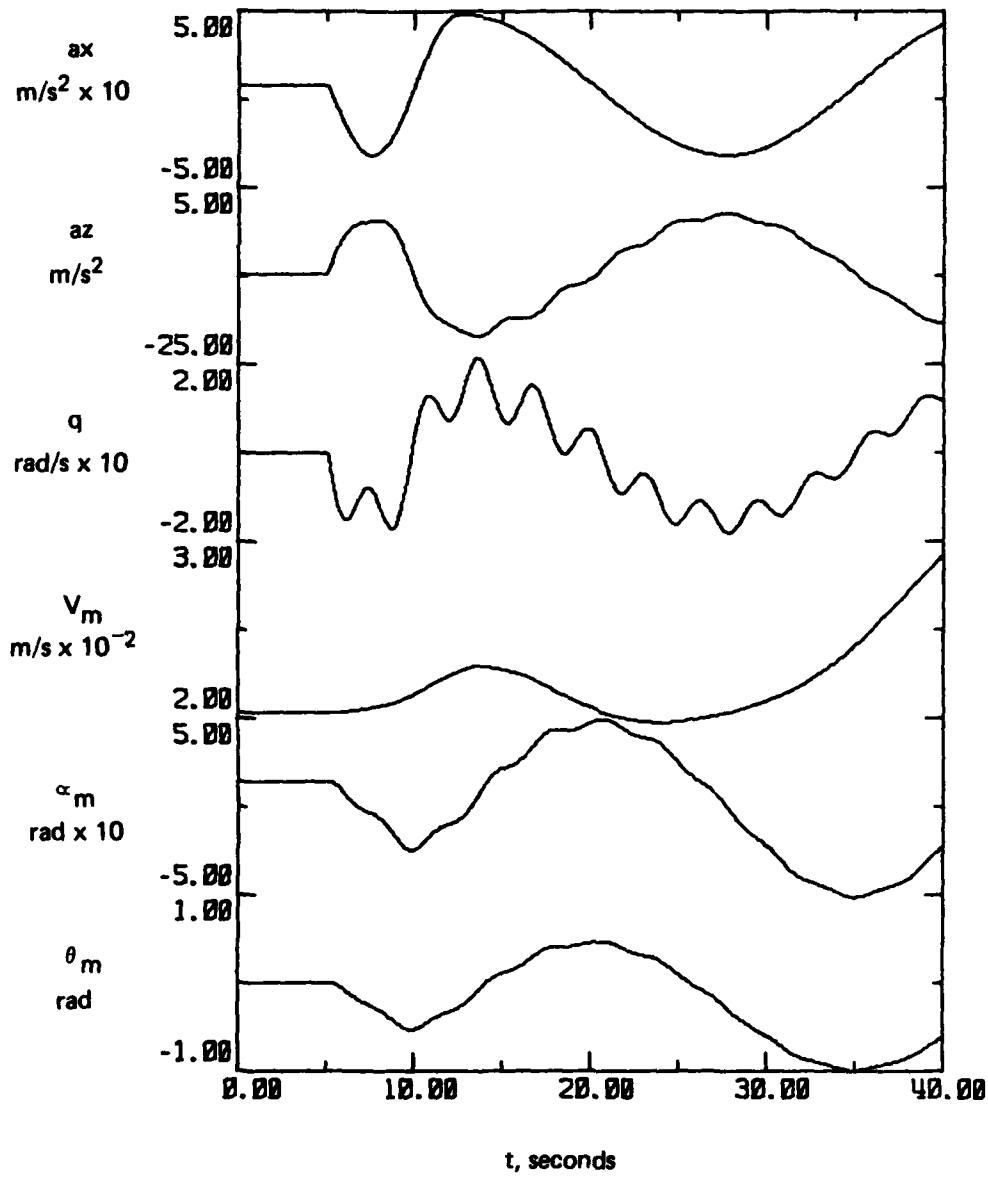

FIG. 1 MANOEUVRE 1 TIME HISTORIES

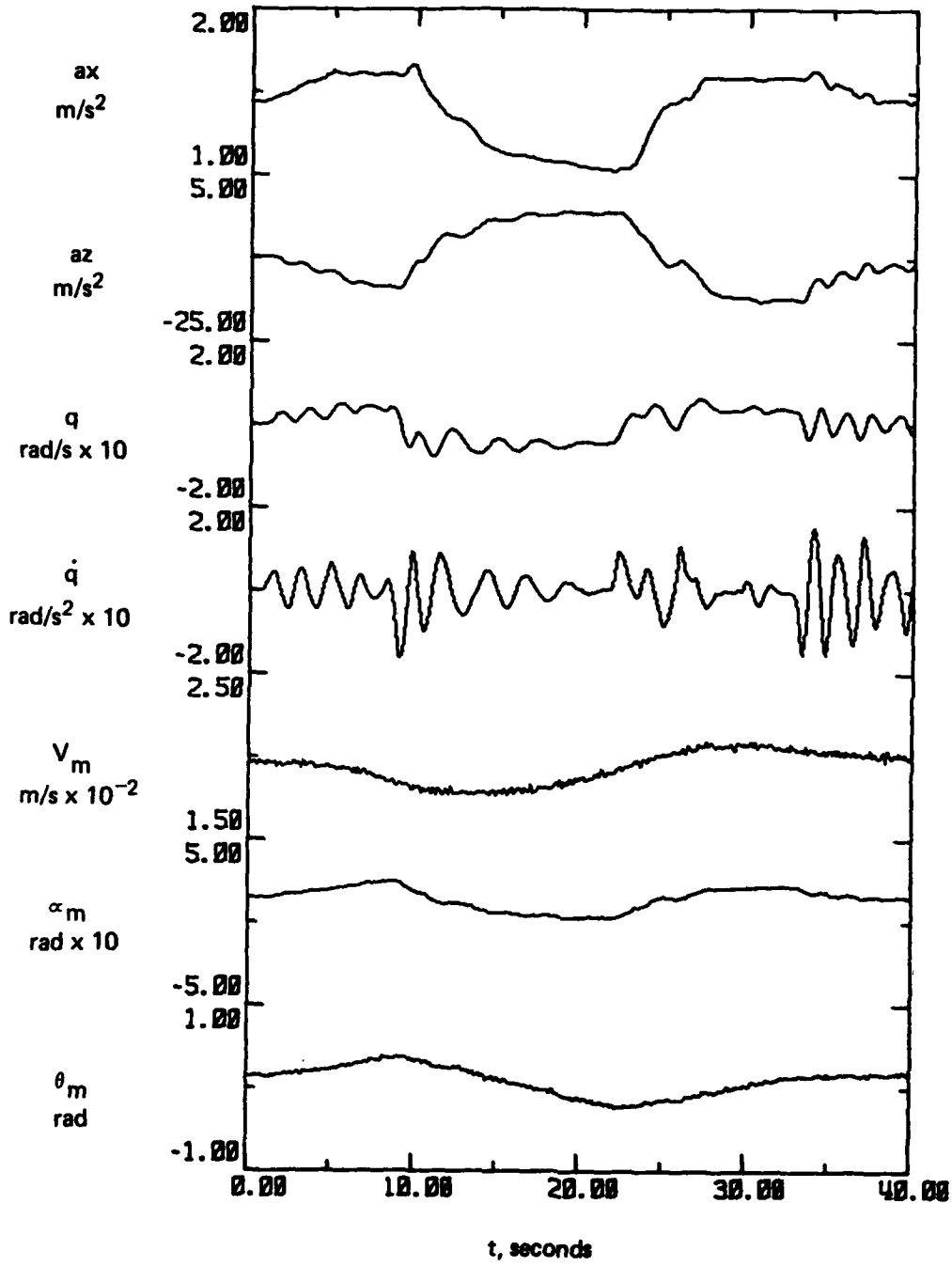

FIG. 2 MANOEUVRE 2 TIME HISTORIES

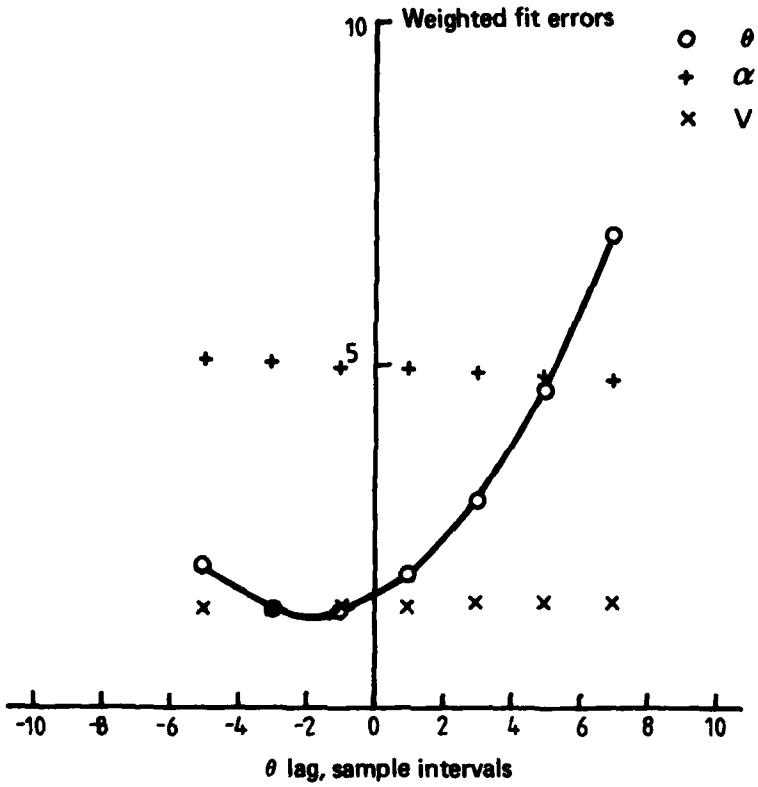

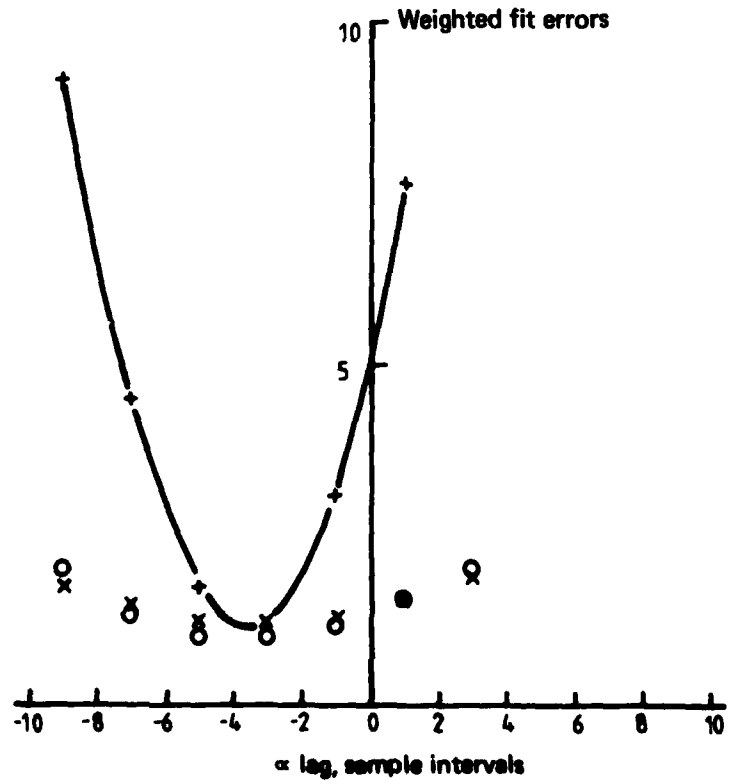

FIG. 3 LAG DETERMINATION IN θ, α RECORDS – SIMULATED DATA

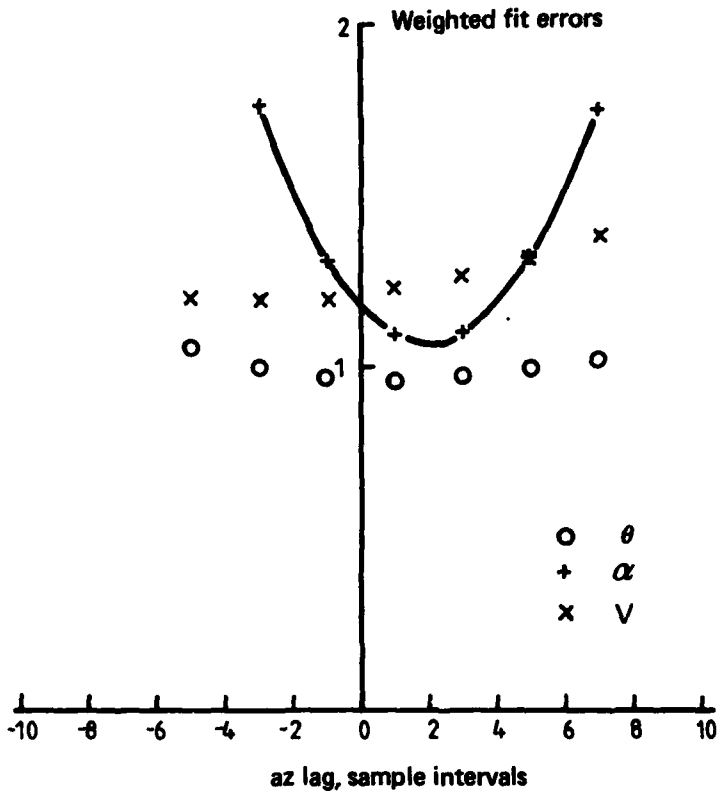

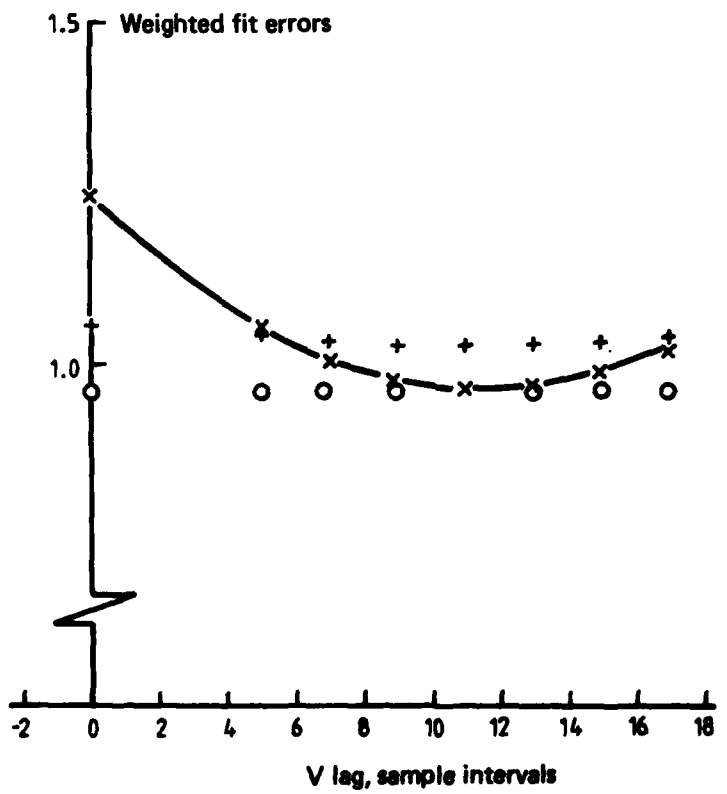

FIG. 4 LAG DETERMINATION IN az,V RECORDS – SIMULATED DATA

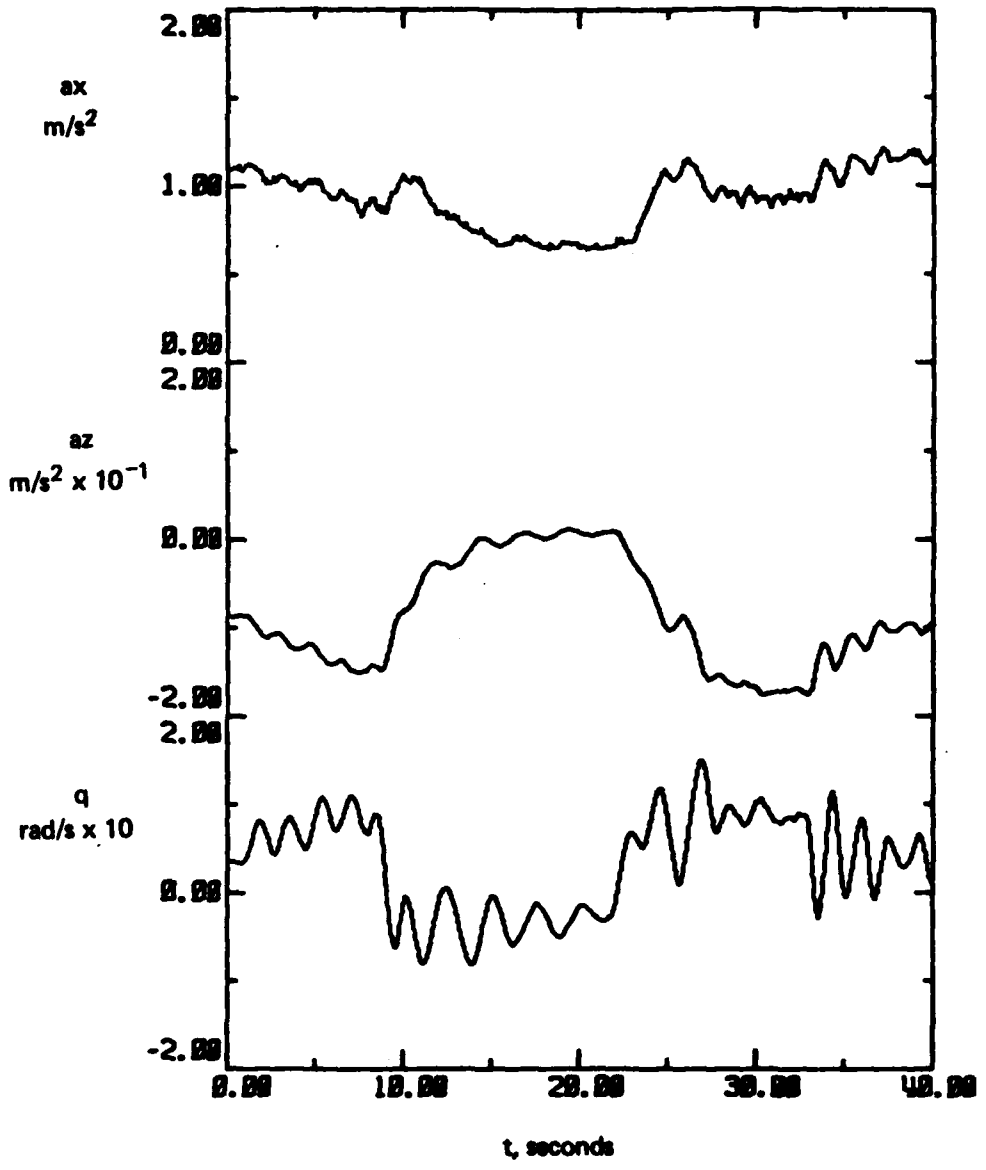

FIG. 5 INPUT TIME HISTORIES – FLIGHT DATA

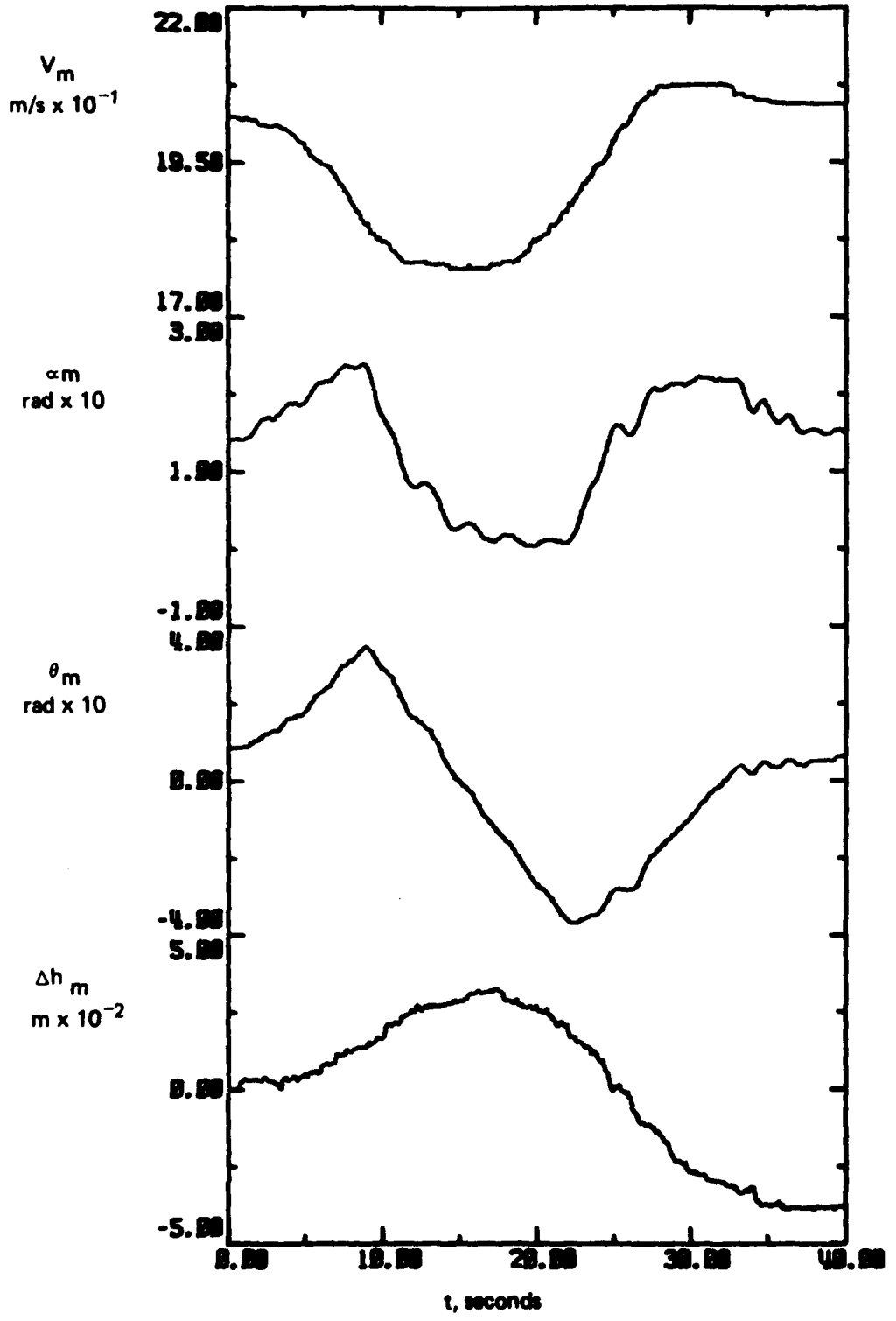

FIG. 5 (cont.) OUTPUT TIME HISTORIES – FLIGHT DATA

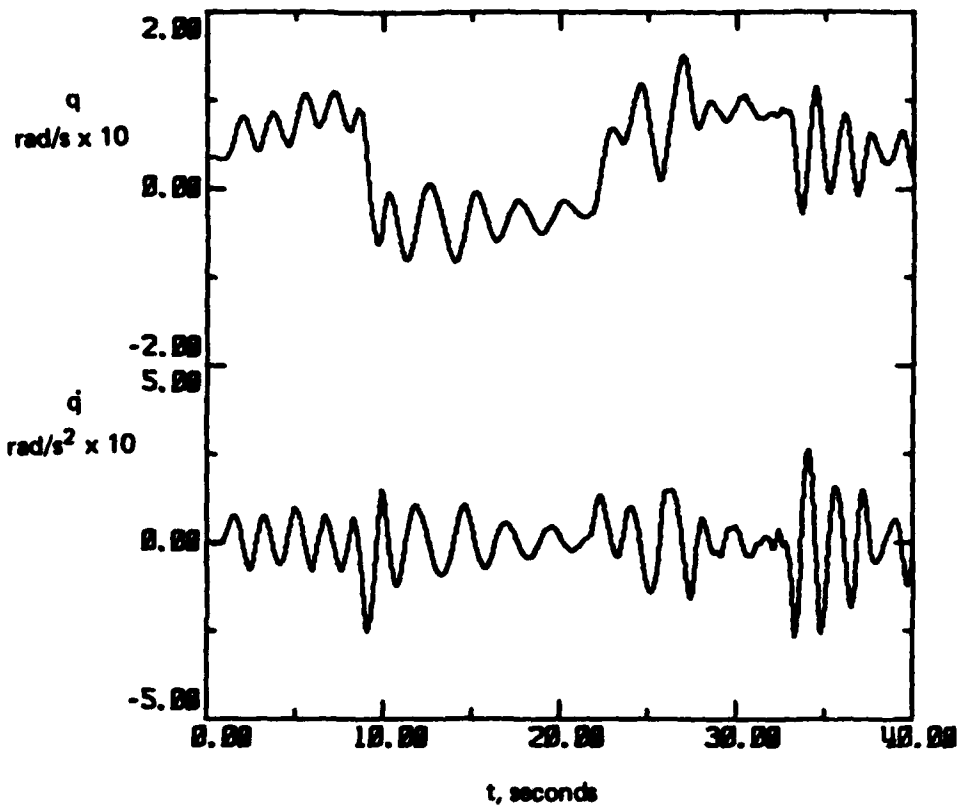

FIG. 6 PITCH RATE AND ACCELERATION HISTORIES

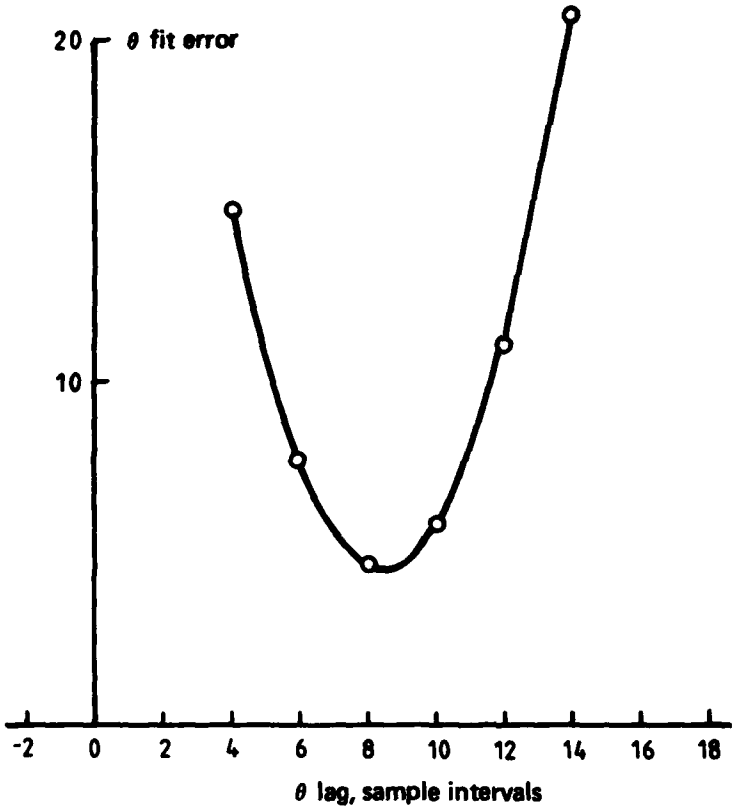

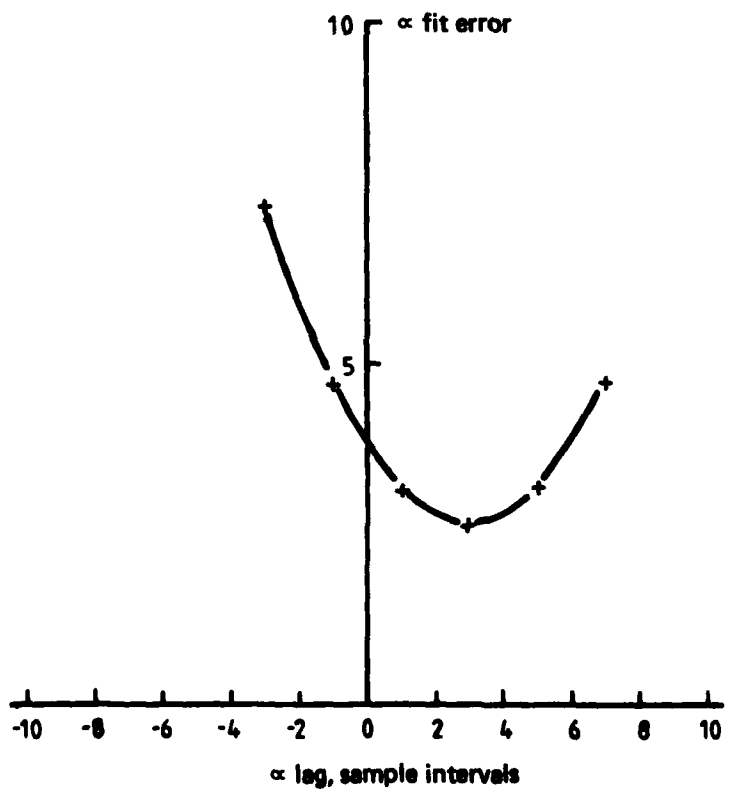

FIG. 7 LAG DETERMINATION IN θ, α RECORDS – FLIGHT DATA

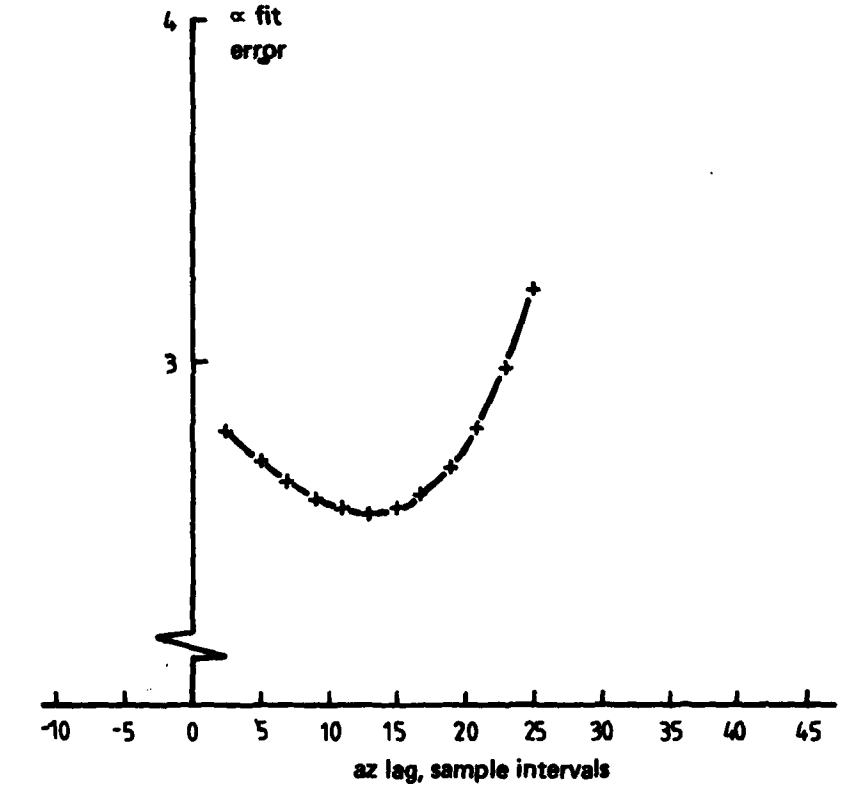

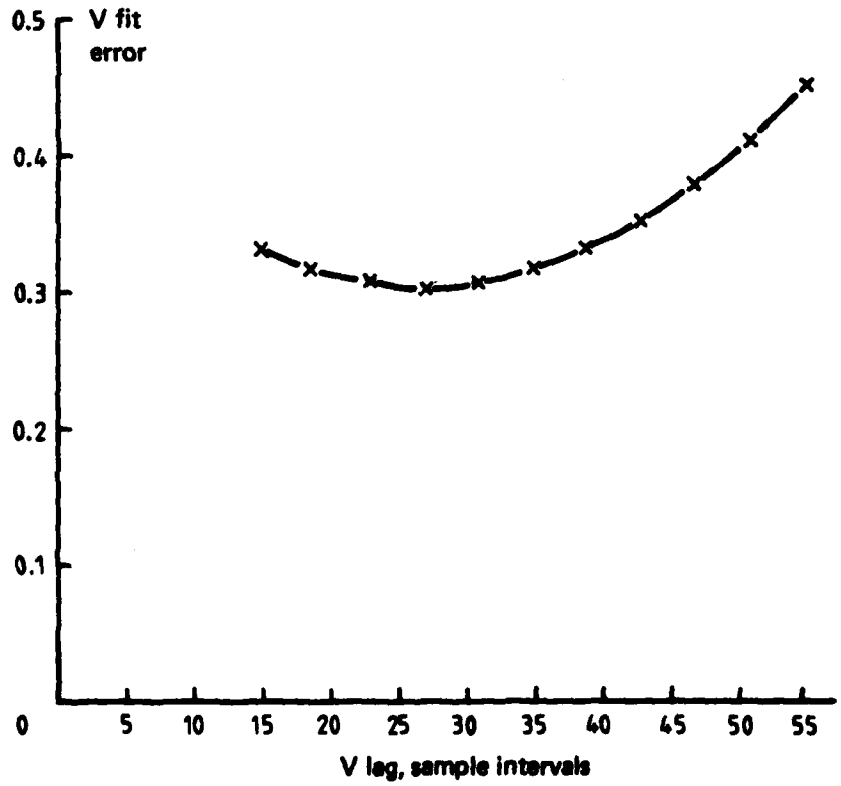

FIG. 8 LAG DETERMINATION IN α, V RECORDS – FLIGHT DATA

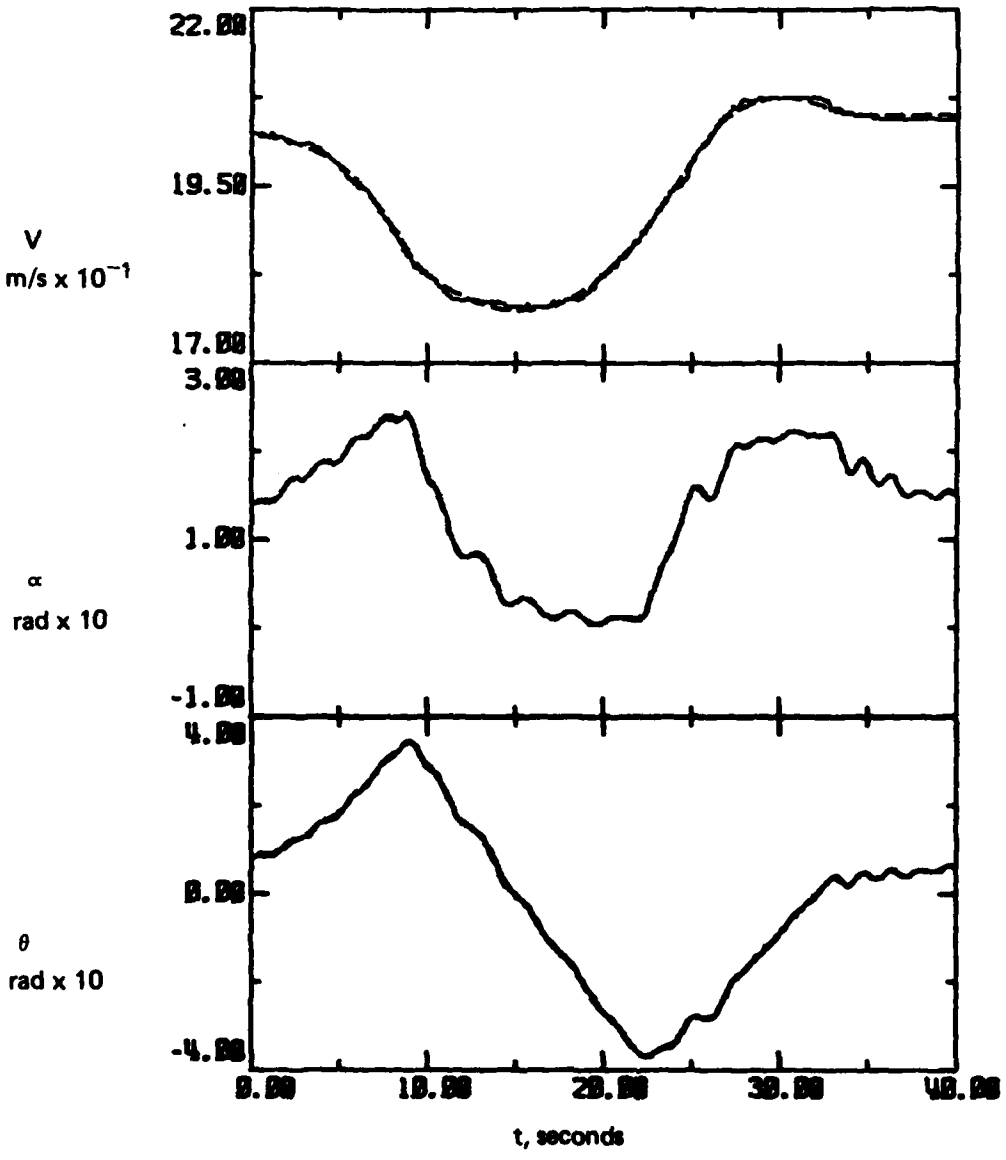

FIG. 9 COMPARISON OF MEASURED AND CALCULATED HISTORIES

DISTRIBUTION

AUSTRALIA

DEPARTMENT OF DEFENCE

Central Office

Chief Defence Scientist
Deputy Chief Defence Scientist
Superintendent, Science and Program Administration
Controller, External Relations, Projects and Analytical Studies
} (1 copy)
Defence Science Adviser (U.K.) (Doc. Data sheet only)
Counsellor, Defence Science (U.S.A.) (Doc. Data sheet only)
Defence Science Representative (Bangkok)
Defence Central Library
Document Exchange Centre, D.I.S.B. (18 copies)
Joint Intelligence Organisation
Librarian H Block, Victoria Barracks, Melbourne
Director General—Army Development (NSO) (4 copies)

Aeronautical Research Laboratories

Director
Library
Superintendent—Aerodynamics
Divisional File—Aerodynamics
Author: R. A. Feik
D. A. Secomb
C. A. Martin
A. J. Farrell
C. R. Guy
N. E. Gilbert
D. A. H. Bird
T. G. Ryall

Materials Research Laboratories

Director/Library

Defence Research Centre

L. M. Sheppard, WSRL
Library

Navy Office

Navy Scientific Adviser
Directorate of Naval Aircraft Engineering

Army Office

Scientific Adviser—Army

Air Force Office

Air Force Scientific Adviser
Aircraft Research and Development Unit
Scientific Flight Group
Library
Technical Division Library
Director General Aircraft Engineering—Air Force
HQ Support Command (SLENGO)
RAAF Academy, Point Cook

DEPARTMENT OF DEFENCE SUPPORT

Government Aircraft Factories

Manager
Library
W. Kidd
D. Pilkinston

STATUTORY AND STATE AUTHORITIES AND INDUSTRY

Commonwealth Aircraft Corporation, Library
Hawker de Havilland Aust. Pty Ltd, Bankstown, Library

UNIVERSITIES AND COLLEGES

Melbourne	Engineering Library
Monash	Hargrave Library
Newcastle	Library Professor G. C. Goodwin Dr R. J. Evans
Sydney	Engineering Library Professor G. A. Bird
N.S.W.	Physical Sciences Library Professor R. A. A. Bryant, Mechanical Engineering
R.M.I.T.	Library

CANADA

NRC, Aeronautical and Mechnaical Engineering Library

FRANCE

ONERA, Library

GERMANY

DFVLR Braunschweig, Mr J Kaletka

INDIA

National Aeronautical Laboratory, Information Centre

NETHERLANDS

National Aerospace Laboratory (NLR), Library

Universities

Delft University
of Technology J. A. Mulder

UNITED KINGDOM

Royal Aircraft Establishment
Bedford
Library
Farnborough
A. Jean-Ross
Library

Universities and Colleges

Cranfield Institute
of Technology Library

UNITED STATED OF AMERICA

NASA Scientific and Technical Information Facility
NASA Dryden, K. W. Iliff
NASA Langley
V. Klein
L. W. Taylor
Library

SPARES (10 copies)

TOTAL (100 copies)

Department of Defence

DOCUMENT CONTROL DATA

1. a. AR No.	1. b. Establishment No.	2. Document Date	3. Task No.
AR-003-931	ARL-AERO-R-161	June 1984	DST 82/031

4. Title	5. Security	6. No. Pages
ON THE APPLICATION OF COMPATIBILITY CHECKING TECHNIQUES TO DYNAMIC FLIGHT TEST DATA	a. document: Unclassified b. title: U c. abstract: U	25 7. No. Refs: 12

8. Author(s)	9. Downgrading Instructions
R. A. Feik	—

10. Corporate Author and Address	11. Authority (as appropriate)
Aeronautical Research Laboratories PO Box 4331, Melbourne, Vic., 3001	a. Sponsor c. Downgrading b. Security d. Approval

12. Secondary Distribution (*of this document*)
Approved for Public Release

Overseas enquirers outside stated limitations should be referred through ASDIS, Defence Information Services Branch, Department of Defence, Campbell Park, CANBERRA, ACT, 2601.

13. a. This document may be ANNOUNCED in catalogues and awareness services available to . . .
No Limitations

13. b. Citation for other purposes (*i.e. casual announcement*) may be (select) unrestricted (or) as for 13 a.

14. Descriptors		15. COSATI Group
Non-linear Systems	Flight Path Reconstruction	01040
Flight tests	Maximum Likelihood estimates	
Data acquisition	Instrument Errors	
Estimation	Time lag	
System identification		

16. Abstract

This note considers matters related to the application of instrument compatibility checking techniques to flight test data. A previously developed Maximum Likelihood program has been used to study the effects of the presence of scale errors, accelerometer offsets and measurement time lags using simulated data. Some additional information on the effects of noise levels has also been obtained. The results have led to a suggested method for determination of centre of gravity location from flight data. The effects of measurement lags have been shown to have a major influence on extracted instrument parameters and a systematic procedure for the determination of relative phases has been devised and applied successfully to simulated data. These techniques have also been applied to flight data from a roller-coaster manoeuvre and a set of relative lag values clearly identified. The question of the accuracies of extracted instrument parameters and their dependence on the relative lags will be treated more fully in a subsequent publication.

Keywords: —

This page is to be used to record information which is required by the Establishment for its own use but which will not be added to the DISTIS data base unless specifically requested.

16. Abstract (*Contd*)

17. Imprint

Aeronautical Research Laboratories, Melbourne.

18. Document Series and Number	19. Cost Code	20. Type of Report and Period Covered
Aerodynamics Report 161	527770	

21. Computer Programs Used

COMPAT.HM, DERIV.HM, SENS.HM (All Fortran)

22. Establishment File Ref(s)

A2/16, A2/51

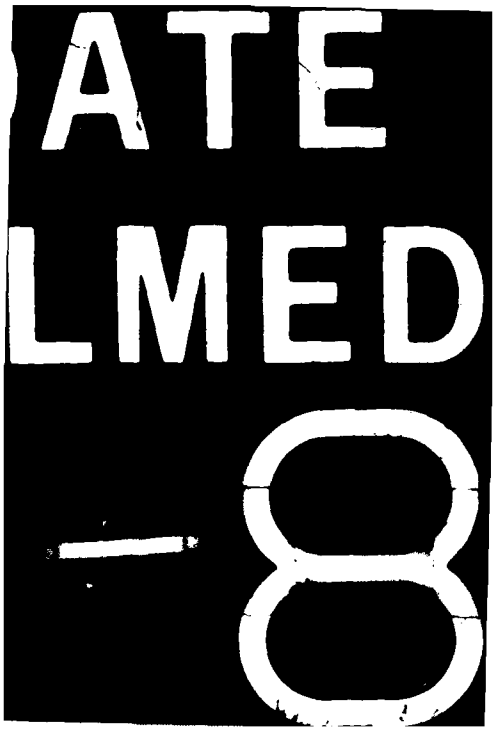
ATE
LMED
8